Planetary and Space Science 138 (2017) 44–54

Contents lists available at ScienceDirect

Planetary and Space Science

journal homepage: www.elsevier.com/locate/pss

Initial SAM calibration gas experiments on Mars: Quadrupole mass spectrometer results and implications

Heather B. Franz[a,b,*], Melissa G. Trainer[b], Charles A. Malespin[b,d], Paul R. Mahaffy[c], Sushil K. Atreya[e], Richard H. Becker[f], Mehdi Benna[a,b], Pamela G. Conrad[b], Jennifer L. Eigenbrode[b], Caroline Freissinet[a,b], Heidi L.K. Manning[g], Benito D. Prats[b,h], Eric Raaen[b], Michael H. Wong[e]

[a] Center for Research and Exploration in Space Science & Technology, UMBC, NASA Goddard Space Flight Center, Greenbelt, MD 20771, United States
[b] Planetary Environments Laboratory, NASA Goddard Space Flight Center, Greenbelt, MD 20771, United States
[c] Solar System Exploration Division, NASA Goddard Space Flight Center, Greenbelt, MD 20771, United States
[d] Goddard Earth Sciences Technology and Research, USRA, NASA Goddard Space Flight Center, Greenbelt, MD 20771, United States
[e] Department of Climate and Space Sciences, University of Michigan, Ann Arbor, MI 48109, United States
[f] School of Physics and Astronomy, University of Minnesota, Minneapolis, MN 55455, United States
[g] Concordia College, Moorhead, MN 56562, United States
[h] SGT, Inc., Greenbelt, MD 20770, United States

ARTICLE INFO

Keywords:
Mars
Atmosphere
Isotopes
Mars Science Laboratory
Sample Analysis at Mars Investigation
Calibration

ABSTRACT

The Sample Analysis at Mars (SAM) instrument suite of the Mars Science Laboratory (MSL) Curiosity rover is equipped to analyze both martian atmospheric gases and volatiles released by pyrolysis of solid surface materials, with target measurements including chemical and isotopic composition (Mahaffy et al., 2012). To facilitate assessment of instrument performance and validation of results obtained on Mars, SAM houses a calibration cell containing CO_2, Ar, N_2, Xe, and several fluorinated hydrocarbon compounds (Franz et al., 2014; Mahaffy et al., 2012). This report describes the first two experiments utilizing this calibration cell on Mars and gives results from analysis of data acquired with the SAM Quadrupole Mass Spectrometer (QMS). These data support the accuracy of isotope ratios obtained with the QMS (Conrad et al., 2016; Mahaffy et al., 2013) and provide ground-truth for reassessment of analytical constants required for atmospheric measurements, which were reported in previous contributions (Franz et al., 2015, 2014). The most significant implication of the QMS data involves reinterpretation of pre-launch contamination previously believed to affect only CO abundance measurements (Franz et al., 2015) to affect N_2 abundances, as well. The corresponding adjustment to the N_2 calibration constant presented here brings the atmospheric volume mixing ratios for Ar and N_2 retrieved by SAM into closer agreement with those reported by the Viking mission (Owen et al., 1977; Oyama and Berdahl, 1977).

1. Introduction

The Sample Analysis at Mars (SAM) instrument suite, which includes a Quadrupole Mass Spectrometer (QMS), Gas Chromatograph (GC), and Tunable Laser Spectrometer (TLS), was designed to perform precise in situ measurements of the chemical and isotopic composition of the martian atmosphere and volatiles associated with surface materials (Mahaffy et al., 2012; Webster and Mahaffy, 2011). SAM measurements of volume mixing ratios (VMR) for the most abundant martian atmospheric species were initially computed with empirical calibration constants derived from pre-launch data (Franz et al., 2014). These constants were later revised on the basis of laboratory experiments and instrument performance during the first Mars year of SAM operations (Franz et al., 2015). The later report described enhanced modeling of instrument background, pressure-related behavior, and mass interferences that improved calculations of VMR for the minor atmospheric species O_2 and CO. At the time of its publication, explanation for the difference in ratio of Ar to N_2 obtained by SAM (Mahaffy et al., 2013) and Viking (Owen et al., 1977; Oyama and Berdahl, 1977) remained an outstanding question of interest, but prior to execution of the calibration cell experiment, insufficient data were available to assign this difference to a SAM instrument effect with confidence (Franz et al., 2015).

The first two experiments utilizing the SAM calibration cell on Mars

* Correspondence to: Center for Research and Exploration in Space Science & Technology, UMBC, NASA Goddard Space Flight Center, Code 699, Greenbelt, MD 20771, United States.
E-mail address: heather.b.franz@nasa.gov (H.B. Franz).

http://dx.doi.org/10.1016/j.pss.2017.01.014
Received 2 December 2016; Accepted 26 January 2017
Available online 27 January 2017
0032-0633/ Published by Elsevier Ltd.

were performed in July and December 2015 (on MSL mission Sols 1042 and 1204) and designated SAM experiments #25274 and #25321, respectively. For simplicity in this manuscript, we will refer to them as CG1 and CG2 (i.e., Calibration Gas 1 and 2). These experiments provided opportunities to assess the continued robustness of the calibration constants through their application to a gas mixture of known chemical and isotopic composition. Results of QMS analysis of the calibration gas suggested a need to update the constant required for calculation of atmospheric N_2 abundance, while indicating accurate retrieval of CO_2 and Xe isotope ratios.

SAM experiment design and analysis are supported by efforts using laboratory facilities at the NASA Goddard Space Flight Center (GSFC). The SAM breadboard and test bed models incorporate quadrupole mass spectrometers fabricated at GSFC to the same design as the flight model and controlled with identical electronics and flight software, rendering these instruments high-fidelity facsimiles of SAM. The breadboard employs the SAM prototype QMS in a laboratory setting that allows flexibility in plumbing configuration for a range of experiments supporting both atmospheric and solid sample analyses. The test bed comprises a replica of SAM, including all instrument and gas processing system components. The test bed is housed in an environmental chamber that simulates martian ambient conditions. All experiments executed on Mars, including those using the calibration cell, are first performed on the SAM test bed for script validation. For the studies described here, both instruments utilized operating parameters analogous to those of the flight model as implemented in ground calibration or on Mars.

2. QMS calibration

The following subsections about SAM QMS calibration provide context for the calibration gas experiments but are not intended to represent a comprehensive discussion. The reader is referred to previous contributions for detailed treatment of the calibration performed prior to these experiments (Franz et al., 2015, 2014).

2.1. Pre-launch calibration

Prior to its integration with Curiosity, the SAM suite was subjected to pre-launch calibration of all components. QMS calibration included tuning of the mass analyzer, derivation of detector correction functions, and determination of empirical calibration constants for VMR measurements through analysis of calibration gas mixtures of known composition (Franz et al., 2014). These calibration constants effectively account for differences in tuning across the mass range and between regions of different RF frequency that produce differences in number of ions detected for the same absolute abundance, even when differences in ionization efficiency for chemical species are considered. They ultimately allow determination of CO_2, Ar, O_2, N_2 and CO VMR in the martian atmosphere through the ratio of a key "marker" fragment of each molecule to ^{40}Ar and the relationship

$$[X]/[Ar] = F_{Xi/Ar} \cdot c_i / c_{40,} \quad (1)$$

where X is the atmospheric species, $F_{Xi/Ar}$ is the calibration constant for that species at the ion fragment i, and c_i and c_{40} are the counts at mass/charge (m/z) ratio i and 40, respectively (Franz et al., 2014). The marker fragment for each species relevant to the calibration cell experiment is given in Table 2. In addition, relevant constants for CO_2 isotopic measurements were informed by independent analysis of the isotopic composition of CO_2 in the calibration gas mix by dual inlet isotope ratio mass spectrometry on a Thermo Scientific MAT 253 at GSFC (Franz et al., 2014). CO_2 from the same source tank was included in the onboard calibration cell utilized on Mars and described in this manuscript.

Constants derived during pre-launch calibration using an equimolar mixture ("EQ mix") of CO_2, N_2, Ar and O_2 (Franz et al., 2014) were used to calculate the martian atmospheric composition reported in Mahaffy et al. (2013). However, a modification was required for the constant used to calculate CO abundance due to an apparent change in instrument background at m/z 12 (C^+, fragment of CO_2 and CO) on Mars compared to ground calibration (Franz et al., 2014). Because limited data were available to establish the new m/z 12 baseline at that time, only an upper limit for CO abundance was reported by Mahaffy et al. (2013).

2.2. Calibration refinement

After monitoring QMS performance throughout the nominal MSL mission of one Mars year, the SAM team determined that some updates to the calibration constants and data reduction procedures were needed to address minor changes in QMS parameters and instrument artifacts that had arisen since pre-launch calibration. The updates accounted for slight changes in tuning at m/z relevant to atmospheric measurements, pressure-dependent production of CO_2^{++} ions at m/z 22, and oxygen fragments from CO_2 that affect O_2 VMR calculations (Franz et al., 2015). The availability of data covering a full Mars year also allowed better characterization of the change in instrument background at m/z 12, making precise measurements of CO VMR possible (Franz et al., 2015).

An unexpected result of initial SAM atmospheric analyses was the retrieval of $^{40}Ar/^{14}N$ ~0.5 (Mahaffy et al., 2013), which differed from the values of 0.3 and 0.35 reported by the Viking team (Owen et al., 1977; Oyama and Berdahl, 1977). The marker fragment used to compute N_2 VMR is m/z 14 (Franz et al., 2014), comprised of approximately 40% N^+ ions and 60% N_2^{++} ions (Wong et al., 2013). There is also a minor contribution from CO^{++} ions generated from CO and CO_2 in the martian atmosphere, but their abundance compared to ions at m/z 14 sourced from nitrogen is negligible. Calibration performed with pure nitrogen gas on the SAM test bed indicated no pressure effect on N_2^{++} production, as seen with CO_2^{++} ions (Franz et al., 2015). Since the species responsible for the m/z 12 background during ground calibration was not identified, although an organic compound was considered likely, we evaluated the relative behavior of ratios computed between m/z 12, 13 and 14 and m/z 22 and 40 to determine whether a similar change in background might be evident at m/z 14, thus affecting N_2 VMR retrievals (Franz et al., 2014). However, the behavior of these ion fragments alone did not provide sufficient clarity concerning this issue, likely reflecting trace quantites of residual terrestrial N_2 in the system that blurred the trend in ratios involving m/z 14. Further evaluation of the N_2 calibration constant was deferred until execution of calibration gas experiments on Mars (Franz et al., 2015).

3. Calibration gas experiments

3.1. Calibration cell contents

The SAM calibration cell, with volume of 4.76 mL, contains approximately equimolar abundances of CO_2, N_2, Ar and Xe and trace quantities of several fluorinated hydrocarbon compounds (Table 1) (Mahaffy et al., 2012). Xenon in the cell is spiked with excess ^{129}Xe for clear differentiation from indigenous martian Xe. Perfluorotributylamine (PFTBA) provides a standard for mass calibration and sensitivity during QMS tuning. The remaining compounds, 1-fluoronaphthalene (FN), 2,2′-difluoro-1,1′-biphenyl (DFBP), and perfluorobiphenyl (PFBP), serve as additional standards for QMS mass resolution and for relative retention times during gas chromatographic (GC) analyses on columns designed to detect high-molecular weight organic compounds.

3.2. Additional calibration for Xe measurements

Analysis of Xe data from the calibration cell requires application of

Table 1
Calibration cell contents.

Abbreviation	Species	Molecular weight	Volume mixing ratio at 100 °C[a]
CO_2	Carbon dioxide	44	24.32%
N_2	Nitrogen	28	24.10%
Ar	Argon	40	24.04%
Xe_T	Xenon, terrestrial isotopic composition	131	8.48%
^{129}Xe	Xenon, 88.9 atom% ^{129}Xe	129	15.51%
PFTBA	Perfluorotributylamine	671	3.00%
FN	1-fluoronaphthalene	146.161	0.54%
DFBP	2,2′-difluoro-1,1′-biphenyl	190.189	0.016%
PFBP	Perfluorobiphenyl	334.112	0.0078%

[a] Uncertainties are estimated at 1% of stated value.

constants that are not needed for routine atmospheric measurements. These include a calibration constant for VMR calculations and correction factors for mass discrimination, which is significant at Xe masses, and isobaric interferences from fragments of the fluorinated hydrocarbon (F-HC) compounds in the calibration cell for accurate retrieval of isotope ratios.

The calibration constant for calculation of Xe VMR was derived from pre-launch analysis of a gas mixture containing 10 vol% each Ne, Ar, Kr and Xe in balance of He. The ratio of *m/z* 132 and 40, adjusted to account for the ^{129}Xe-spiked composition of Xe in the calibration cell, establishes the calibration constant for Xe, analogous to those for atmospheric species described above and given in Franz et al. (2015). These constants, used for initial analysis of calibration cell data, are listed in the third column of Table 2.

The correction for mass discrimination at Xe isotopes is described in Conrad et al. (2016). Corrections for F-HC interferences were derived from pre-launch experiments that exercised the calibration cell. Because no isobaric interferences from the F-HC compounds were detected at *m/z* 136, and indeed none are expected based on mass spectra from the National Institute of Standards and Technology (NIST), F-HC correction factors were computed from ratios of each Xe isotope to ^{136}Xe, following correction for mass discrimination. The average composition thus observed was compared to that expected for Xe in the calibration cell, and excesses were assigned to F-HC interferences. The observed and expected ratios at Xe-relevant masses are shown in Fig. 1, while the resulting F-HC correction factors, representing the fraction of signal at a given mass attributed to Xe, are provided in Table 3.

The F-HC correction algorithm just described assumes identical operating conditions between the calibration experiments used to derive the F-HC correction and experiments executed on Mars. Because the calibration cell must be heated above 100 °C to ensure that all F-HC components are fully volatilized (Mahaffy et al., 2012), this assumption may not strictly hold for experiments utilizing temperature profiles that differed from those used in ground calibration. During the relevant ground calibration experiments, all manifolds were heated to 135 °C. During the CG1 experiment, however, the manifold containing the calibration cell was heated to 135 °C, while all other manifolds were heated to 50 °C for conservative power usage. During the CG2 experiment, all manifolds were heated to 50 °C to establish an isothermal environment. These temperature differences caused a reduction in abundances of F-HC compounds that reached the QMS, requiring an additional adjustment to Xe data. This adjustment was implemented based on the relative ratios between each Xe-relevant *m/z* and *m/z* 69, which includes fragments from all four F-HC compounds in the calibration cell.

One further difference between ground calibration and flight experiments required consideration when calculating the necessary adjustments to the F-HC correction factors. To protect the secondary electron multiplier detector during these early calibration experiments, the detector was operated at a low voltage (−1900 V) not optimal for science data collection, which produced mass spectra fractionated from those acquired with the nominal operating voltage (−2252 V) used on Mars. Tests with the SAM breadboard QMS provided a correction function, parameterized in terms of the mass difference between a given *m/z* and *m/z* 132, for these two operating conditions:

$$^{m}X_c = 100 \cdot {}^{m}X_o/(100 + 0.0099 \times \Delta m^2 - 0.2151 \cdot \Delta m), \quad (2)$$

where $^{m}X_c$ and $^{m}X_o$ are the voltage-corrected and observed signal at *m/z* m, respectively, for the ground calibration data and Δm = 132–m. This correction specifically addresses variations in QMS response related to the differences in operating parameters utilized in these ground calibration experiments compared to those of CG1 and CG2 and should not be used in other circumstances.

The resulting adjustment factors needed for the CG1 and CG2 experiments, applied to Xe isotope ratios after the mass fractionation and nominal F-HC corrections, are provided in the last two columns of Table 3.

3.3. Experiment descriptions

A schematic diagram of the SAM instrument suite is shown in Fig. 2. Instrument components and QMS operating modes for atmospheric analyses are discussed in detail elsewhere (Franz et al., 2015, 2014; Mahaffy et al., 2012). Techniques employed for execution and data processing of the calibration gas experiments were generally similar to those described in the preceding references, with some modifications unique to the nature of these analyses. The calibration experiments utilized the tank labeled “Cal Gas,” connected to manifold MN3 in the lower portion of Fig. 2. Specific sections of the manifold were isolated by valve operations during experiment execution and are labeled Vol #1–Vol #5 in Fig. 2 to facilitate the following discussion.

Fig. 3 shows the observed signal at marker fragments for major constituents of the calibration gas during CG1 and CG2 to help illustrate experimental procedures. At the start of the CG1 experiment in Mars, the gas manifold containing the calibration cell was heated to 135 °C, while all other manifolds were heated to 50 °C; during the CG2 experiment, all manifolds were heated to 50 °C. The QMS and manifolds were evacuated by the turbomolecular pumps (WRP1 and WRP2), then the manifolds were isolated from the martian environment through closure of valve V05. Initial background scans were performed with the QMS only, followed by scans with the QMS open to the evacuated manifold. Calibration gas was introduced into Vol #1, 3, 4 and 5 by opening valve V36 for 0.02 s.

In the CG1 experiment, SAM pressure monitor readings indicated that an initial pressure of 6.2 mb was achieved in the manifold. Valve V43 was then closed to isolate gas in Vol #1, and valve V09 was opened for 33 s to introduce gas to the TLS for later analysis. A series of volume expansions was then performed to gradually reduce the gas pressure for QMS analysis. For each expansion, with V43 closed, V05 was opened for 11 s to flush the manifolds downstream of V43 with atmospheric gas, after which they were evacuated by WRP2. Valve 21 was

Table 2
Calibration constants used for VMR measurements.[a,b]

Species or ratio	*m/z* value of marker fragment (i)	$F_{Xi/Ar}$[c] for fractional scan data, used for initial data processing	$F_{Xi/Ar}$[c] for fractional scan data, revised based on EQ mix and CG1 data
CO_2	22	161.3 ± 3.3	159.6 ± 3.3
N_2	14	22.10 ± 0.45	30.42 ± 0.77
Xe	132	11.33 ± 0.16	11.33 ± 0.16
O_2	32	1.453 ± 0.013	1.453 ± 0.014

[a] Constants for CO_2 and N_2 are from Franz et al. (2015).
[b] O_2 calibration constant is not used in calibration cell measurements but is included here to indicate updated uncertainty for use in retrieval of martian atmospheric VMR.
[c] See Eq. (1).

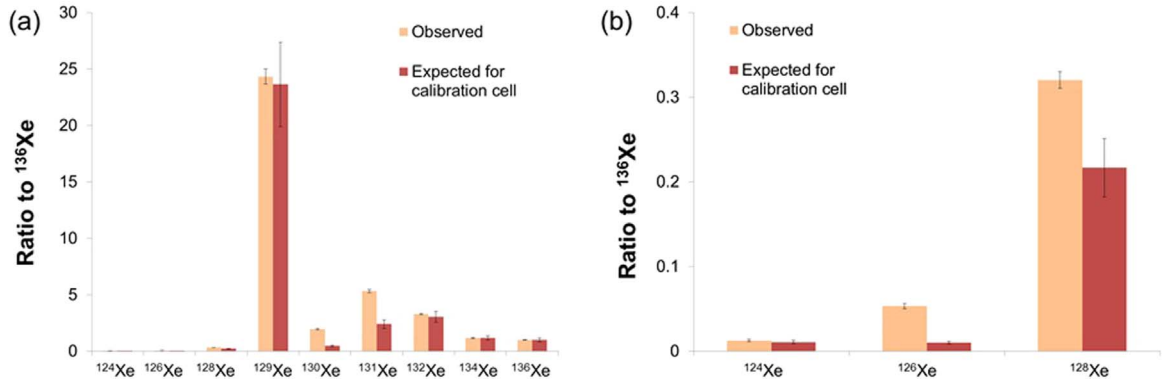

Fig. 1. Pre-flight calibration data used to derive correction factors for isobaric interferences from fluorinated hydrocarbon (F-HC) fragments at Xe masses: (a) All Xe isotopes, (b) Detail of minor isotopes. Excess signal above that expected for the known Xe isotopic composition of the calibration gas was attributed to F-HC fragments.

Table 3
Correction factors for F-HC interferences at Xe masses.

Xe mass	F-HC correction factor	Additional adjustment for observed F-HC abundances relative to ground calibration[a]	
		CG1	CG2
124	0.854 ± 0.162	1.00 ± 0.03	1.09 ± 0.14
126	0.189 ± 0.034	2.20 ± 0.10	3.63 ± 0.43
128	0.677 ± 0.109	0.85 ± 0.02	0.85 ± 0.12
129	0.972 ± 0.156	1.11 ± 0.04	1.09 ± 0.13
130	0.235 ± 0.038	1.00 ± 0.03	0.99 ± 0.14
131	0.451 ± 0.073	1.21 ± 0.03	1.63 ± 0.22
132	0.927 ± 0.148	1.00 ± 0.03	1.00 ± 0.14
134	1.016 ± 0.164	0.94 ± 0.02	0.94 ± 0.13
136	1.000 ± 0.160	0.96 ± 0.02	0.95 ± 0.13

[a] Average values for multiple pressure regimes of each experiment.

subsequently closed and V43 was opened to allow calibration gas to expand into Vol #1, 3 and 4. Each such expansion reduced the gas pressure approximately by half. After each expansion, valve V43 was closed to isolate Vol #1 from the downstream manifolds. While the gas in Vol #1 was analyzed by the QMS, the downstream manifolds were flushed and evacuated to prepare for the next volume expansion. Through this procedure, measurements were performed at pressures of 3.1 mb, 1.5 mb, 0.7 mb, and 0.4 mb, as calculated based on the manifold volumes shown in the table accompanying Fig. 2.

For QMS analyses, gas flowed from the manifold through a glass capillary via valve V11 into the QMS ion source, which utilizes electron impact ionization. During in situ experiments, the QMS scanned a set of *m/z* values that were pre-selected on the basis of the calibration gas composition. This "vector-scanning" approach allowed optimal time resolution for *m/z* of interest (Franz et al., 2014). The QMS scanned for approximately 25 min at each pressure during the CG1 experiment.

Upon completion of the fourth calibration gas analysis, the entire manifold was flushed with martian atmospheric gas and then evacuated. Valve V43 was again closed to isolate Vol #1 from downstream manifolds. A second set of QMS background scans was performed, after which atmospheric gas was introduced to Vol #1 through valve V28. The atmospheric gas was then sampled by the QMS to allow evaluation of atmospheric measurements in the context provided by the preceding calibration analyses.

The second calibration gas experiment (CG2) was performed in December 2015. The experimental design for CG2 included some modifications intended to address complications encountered during processing of CG1 data that suggested unexpected introduction of atmospheric gas to the background during volume expansions, discussed in Section 3.4 below. First, the manifold in Vol #3, 4 and 5 was not flushed with atmospheric gas after each volume expansion, but was simply pumped by WRP2. Second, each analysis segment was increased to approximately 26 min, but only three pressures were sampled in this experiment: 2.9, 1.4 and 0.7 mb (Fig. 3).

3.4. Data processing

Data acquired at each operating pressure were corrected for pressure effects, detector dead time and instrument background by methods similar to those described previously (Franz et al., 2015, 2014). All results utilized integrated peak areas for a given *m/z* ± 0.4 (Franz et al., 2014). A proportional background model was used initially, analogous to that typically employed for analysis of atmospheric gas, with background proportions established by extrapolation of trends observed in the background region at the start of the experiment to the time of calibration gas introduction. Since this gas mixture was processed through each successive volume expansion, the proportions of background and calibration gas were nominally expected to remain constant throughout the calibration measurements.

3.5. VMR calculations

At the highest pressure of each experiment, the signal at *m/z* 40 saturated the QMS detector, so no VMR calculations were possible for those analysis regions. However, volume mixing ratios of the major calibration species (CO_2, Ar, N_2, and Xe) were computed at each subsequent pressure by application of Eq. (1) with the calibration constants given in Table 2. VMR obtained from initial processing of CG1 data did not match the actual calibration gas composition, as shown in Fig. 4(a). In particular, the CO_2 VMR was significantly higher than expected and increased as the calibration gas pressure decreased, while the N_2 VMR was lower than expected. Three possible sources of error were considered: (1) leakage from the calibration cell since loading, (2) inadequate modeling of background contributions during initial data processing, and (3) errors in the calibration constants.

If leakage across the seat of valve V36 that connects the calibration gas cell to the manifold had occurred, mass-dependent fractionation of the gases could have altered the composition of the remaining mixture. The pressure measured during introduction of calibration gas to the manifold in CG1 was in line with the trend established during pre-flight experiments and did not suggest significant leakage from the calibration cell. However, a V36 leak rate of up to 5×10^{-9} atm·cc/s for He was estimated during pre-launch testing. Assuming relative leak rates proportional to the square root of mass of relevant species, the major gas composition of the calibration cell was modeled from the time of loading to its first use on Mars, a period of 2575 days. The model predicted slight decreases in CO_2, N_2 and Ar VMR and a slight increase in Xe VMR, as shown in Fig. 5. Comparison of modeling results in Fig. 5 with VMR results of Fig. 4(a) indicates that a leak of this rate from the calibration cell alone cannot explain the deviations from expected VMR encountered in initial processing of CG1 data.

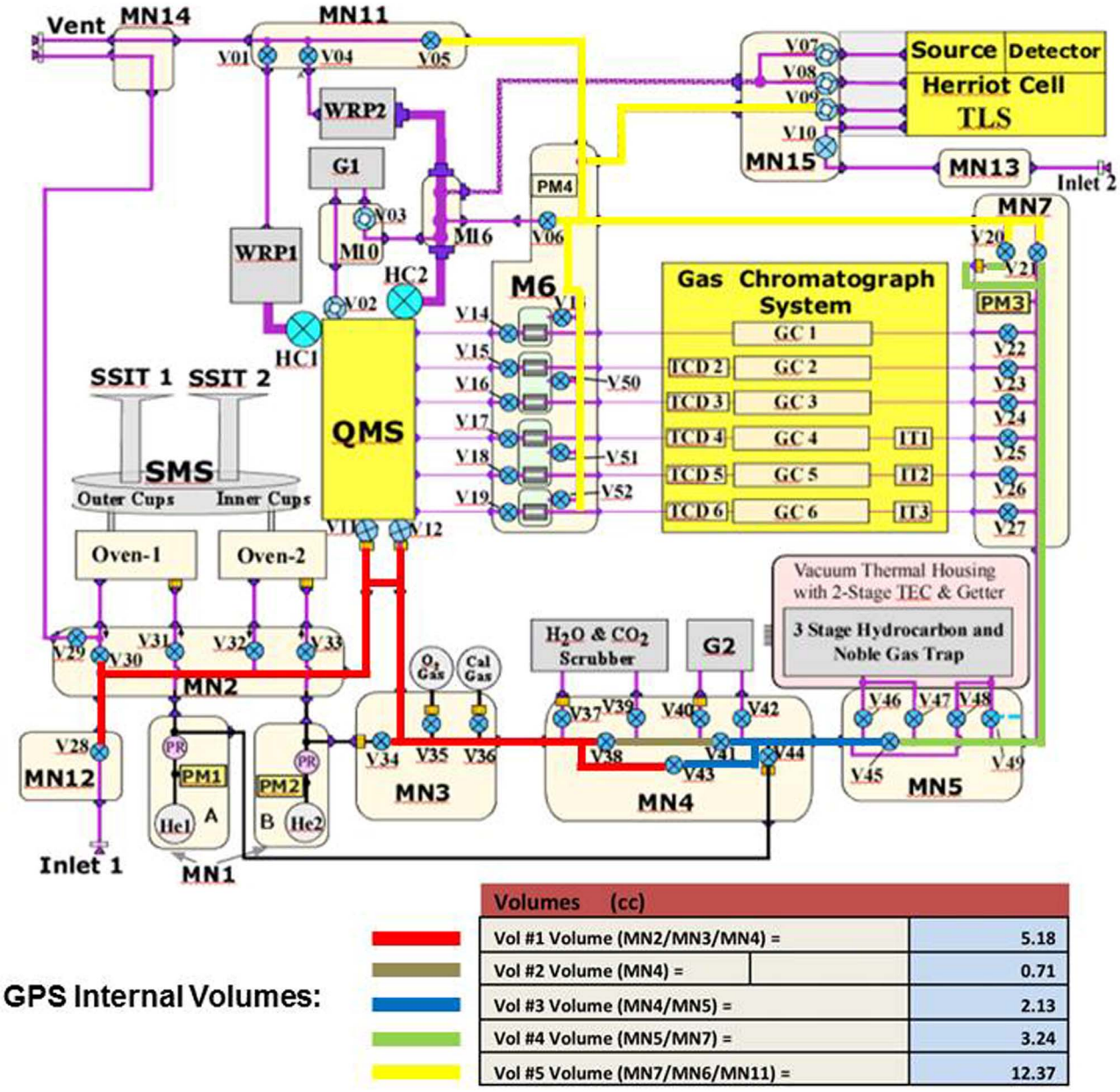

Fig. 2. Simplified schematic of SAM's gas processing system. Isolated volumes relevant to calibration gas experiments are color-coded. (For interpretation of the references to color in this figure legend, the reader is referred to the web version of this article.)

Because the calibration gas in the manifold was below atmospheric pressure during each set of measurements, the apparent excess of CO_2 (Fig. 4(a)) and its pressure dependence suggested that additional background was introduced to the calibration gas during the volume expansions due to atmospheric gas back-streaming through WRP2. This observation prompted redesign of the CG2 experiment to eliminate the atmospheric flushes between volume expansions, but unfortunately this did not eliminate the background issue, as shown in Fig. 4(b).

As CO_2 comprises ~96% of the martian atmosphere, excess CO_2 introduced during volume expansions would dominate VMR calculations, affecting the distribution retrieved for all gases. Thus modeling of excess background gas was crucial to assessment of data from these experiments. It was unknown a priori what proportion of the excess background represented atmospheric gas versus calibration gas that was not fully evacuated from the manifold during pumping, particularly as the composition of the excess gas appeared to vary with manifold pressure. However, an assumption that the background-corrected signal for a known abundance of a given gas should be identical between ground and in situ calibration experiments allowed anchoring of the CG1 and CG2 data to calibrated values. With proper background subtraction, the counts/mb obtained by dividing the signal at the marker fragment of a given gas by the appropriate partial pressure should be constant at every stage of the experiment and should match the counts/mb obtained for the same gas during ground calibration.

Fig. 6 shows the average signal per mb before background subtraction at each marker fragment during the CG1 experiment, as well as the corresponding background-corrected value measured during the EQ mix experiment before launch. It is evident in the figure that the background contribution was generally greater at lower pressures during CG1, particularly for CO_2, the main constituent of the atmosphere. In addition, Fig. 6(c) shows that the observed signal at m/z 14 was below that measured during the EQ mix run. As discussed by Franz et al. (2014, 2015), a shift in QMS sensitivity at m/z 12 compared to pre-launch calibration was observed during atmospheric experiments after landing on Mars and was attributed to a contaminant that affected the ion source region during calibration experiments. Franz et al. (2014,

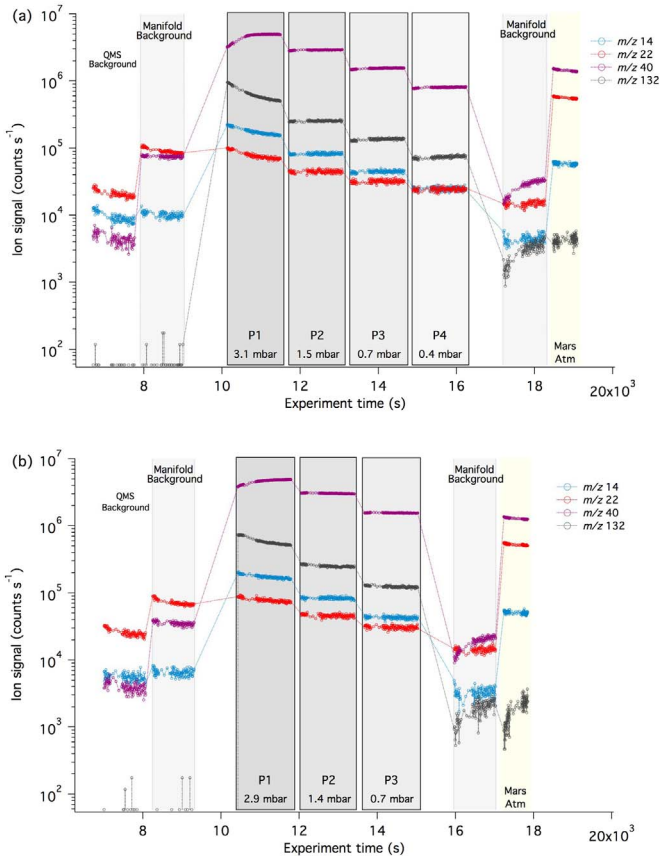

Fig. 3. QMS signal observed at marker fragments for major calibration gas constituents. (a) CG1, (b) CG2. The curve in the m/z 40 trace in the P1 region indicates detector saturation, thus no VMR calculations are performed for this pressure regime.

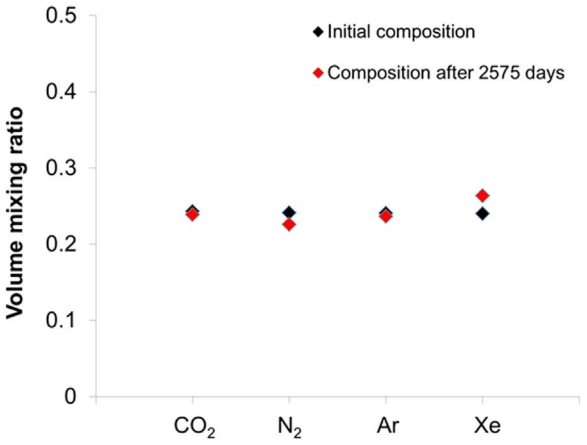

Fig. 5. Calibration cell composition modeled assuming leak rate across V36 of 5×10^{-9} atm·cc/s for He and mass-dependent fractionation of calibration gases for 2575 days after cell loading. Error bars are smaller than the symbols.

2015) considered the possibility that fragments of the same contaminant may have also affected m/z 14, leading to erroneous results for N_2 VMR determined for the martian atmosphere (Mahaffy et al., 2013). The data presented in Fig. 6(c) provide evidence supporting this possibility. After modeling of the nominal proportional background, the average signal observed at m/z 14 during the highest pressure stage of CG1, which incurred minimal contribution from excess background, was used as the target value for m/z 14 signal in the following analysis, with a corresponding adjustment to the N_2 calibration constant.

Based on the known calibration cell composition, subtraction of the background at each species required to achieve the target pressure-normalized QMS signal established by EQ mix data allowed evaluation of the calibration constants. This was accomplished in the following manner. At each pressure in the CG1 and CG2 experiments, the appropriate background signal was subtracted from marker fragments for CO_2, N_2 and Ar to achieve the adjusted counts/mb from ground calibration, as just described. The background signal for Xe was determined as that required to achieve the expected Xe VMR for the calibration gas after correction for contributions from F-HC compounds and adjustment for F-HC abundances compared to ground calibration as discussed in Section 3.2, then the resulting VMR for CO_2, N_2 and Ar were evaluated. As shown in Fig. 7, the calibration constants, after appropriate adjustment to the N_2 calibration constant, retrieved the expected composition of the calibration cell within estimated uncertainties. However, small discrepancies in the expected VMR remained even after this modification. With the initial background issues largely resolved, a leak from the calibration cell and uncertainties in calibration gas composition were investigated as possible sources of these small discrepancies.

Data for CG1 and CG2 do not indicate a He leak rate of 5×10^{-9} atm·cc/s across V36, as shown in Fig. 6, because the observed signal at m/z 132 was insufficient to support Xe VMR of ~27% as predicted by the leak model. The maximum leak allowed by the data is constrained by the observed m/z 132 signal before background subtraction, which for the P2 region of CG1 would yield approximately 24.6% Xe. Our leak model estimates that this Xe VMR would be produced by a He leak of 8.2×10^{-10} atm·cc/s. However, when results of this model were applied to VMR calculations for the calibration cell using the method just described, the VMR retrieved displayed similar

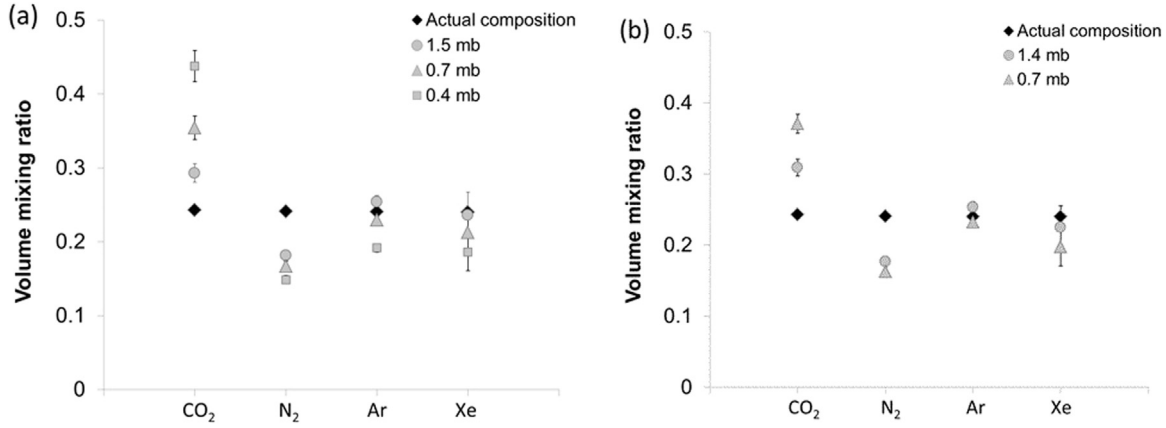

Fig. 4. Volume mixing ratios obtained from initial processing of calibration gas experiments using Eq. (1) and the calibration constants given in Table 1. (a) Experiment CG1, July 2015. (b) Experiment CG2, December 2015.

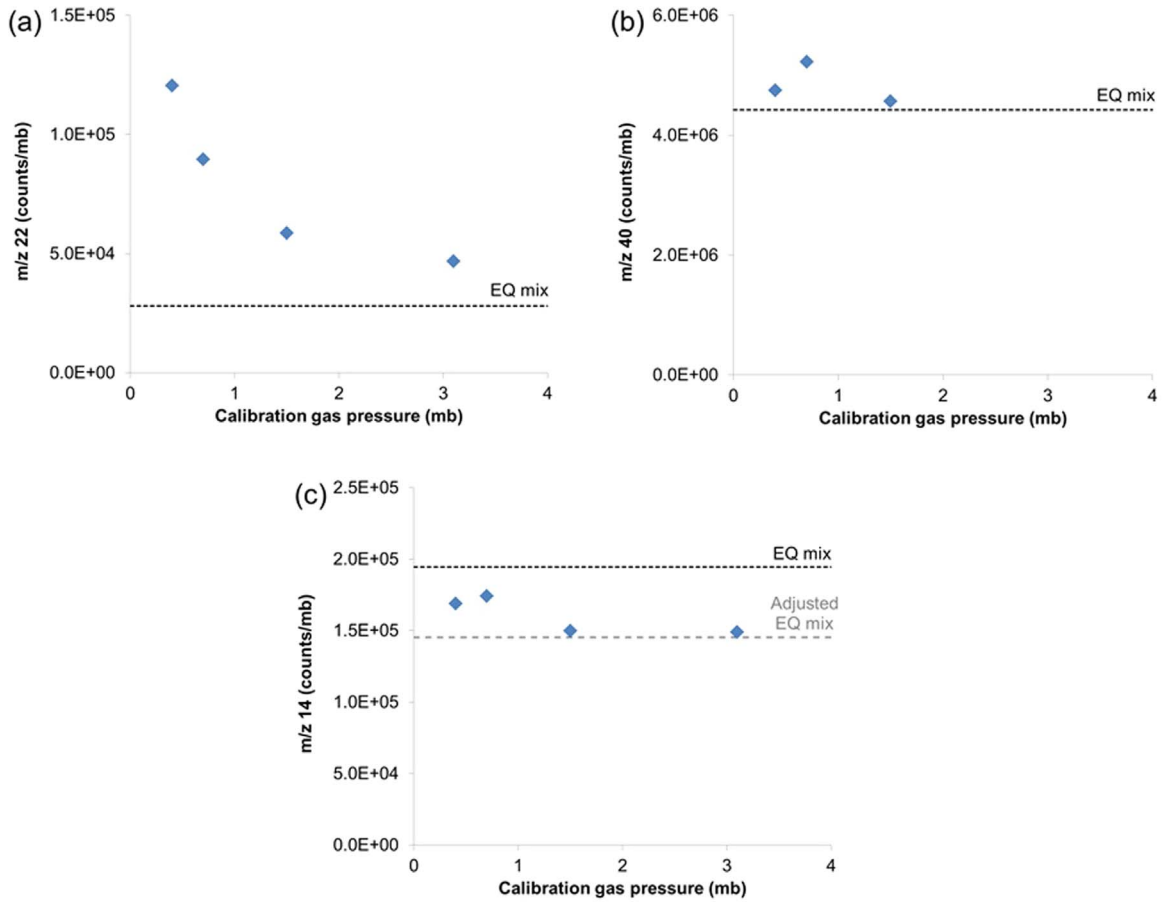

Fig. 6. CG1 experiment – dashed lines show targets for background-subtracted signal at marker fragments of (a) CO_2, (b) Ar, and (c) N_2 (in counts/mb, partial pressures) derived from the equimolar mix ("EQ mix") pre-launch calibration experiment (Franz et al., 2014). Points show the average signal at *m/z* 22, 40 and 14 at each pressure before background subtraction, indicating that the background contribution was greater at lower pressures during CG1. Error bars are smaller than the symbols. As shown in (c), the observed signal at *m/z* 14 before background subtraction was below that measured during the EQ mix run before launch. The "adjusted EQ mix" line represents the average EQ mix signal adjusted by a factor of 1.34 to coincide with the *m/z* 14 signal observed at the start of CG1 after nominal background subtraction.

discrepancies compared to the leak model targets as those compared to the nominal targets shown in Fig. 7. This finding suggested possible deviations between expected and observed calibration gas composition as the source of the discrepancies.

With the analytical method described above, deviations in either the EQ mix or calibration cell composition from that expected would produce apparent errors in VMR retrieved for the calibration cell. In adjusting the calibration constants, we implicitly assume that the EQ mix composition as sampled by the QMS during ground calibration was somewhat different from that documented in Mahaffy et al. (2012). This situation could have arisen, for example, through introduction of a small amount of air to the system during analysis of the EQ mix tank. Assuming validity of the Xe calibration constants, adjustments to the EQ mix composition and resulting calibration constants for CO_2, N_2 and Ar as required to yield the expected calibration cell VMR for CG1 and CG2 were determined. These calculations indicated that a contribution from terrestrial air of approximately 0.2 to 1.2% during EQ mix analysis could be largely responsible for the small discrepancies in calibration

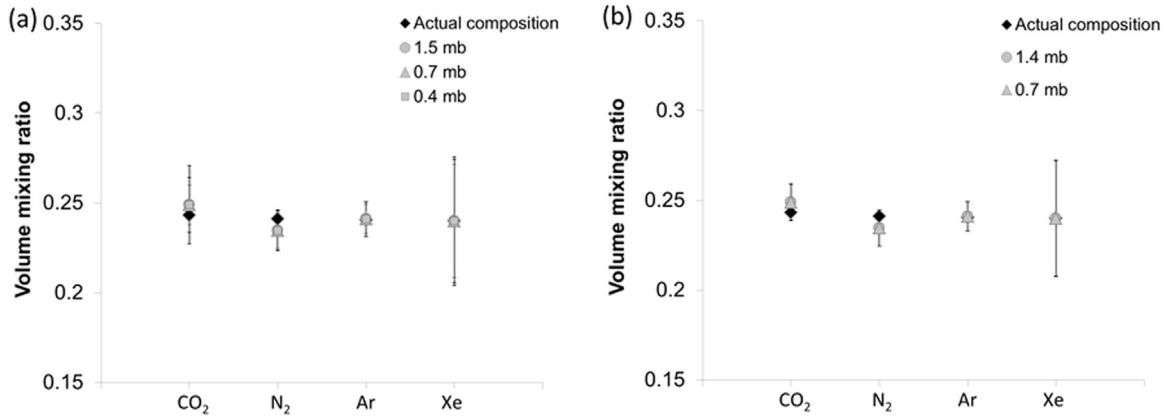

Fig. 7. Volume mixing ratios obtained for the calibration gas after background subtraction targeted to achieve the pressure-normalized signal measured during ground calibration. (a) CG1, (b) CG2.

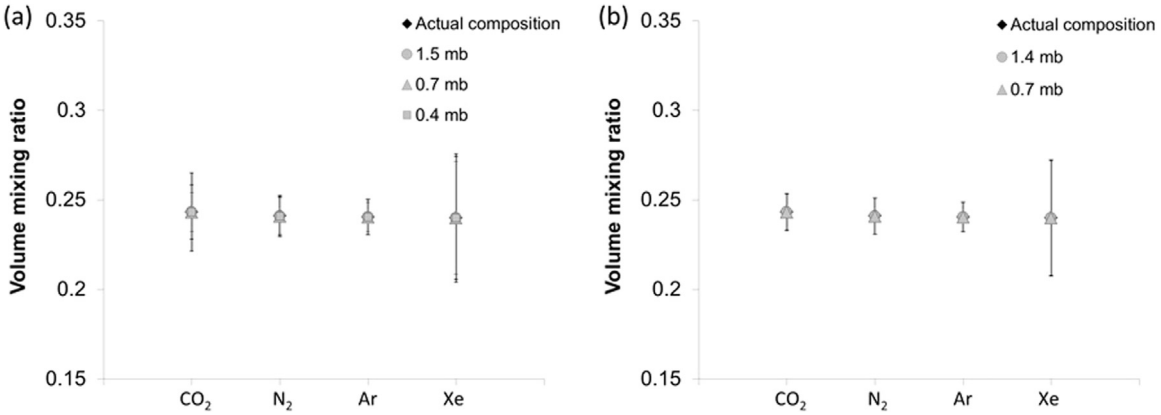

Fig. 8. VMR obtained with calibration constants modified on assumption of deviations between expected and measured EQ mix composition during derivation of original constants, as well as the adjustment to the N_2 calibration constant to address effects of a filament contaminant inferred to be present during early experiments on Earth and Mars.

Table 4
Effects of applying revised calibration constants to VMR calculations for CG1 and CG2.

Species	Actual	CG1			CG2	
	VMR	P2	P3	P4	P2	P3
CO_2	0.2432	0.2432 (± 0.0112)	0.2432 (± 0.0154)	0.2432 (± 0.0218)	0.2432 (± 0.0103)	0.2432 (± 0.0106)
N_2	0.2410	0.2409 (± 0.0106)	0.2410 (± 0.0118)	0.2410 (± 0.0121)	0.2410 (± 0.0107)	0.2409 (± 0.0106)
Ar	0.2404	0.2404 (± 0.0086)	0.2404 (± 0.0100)	0.2404 (± 0.0100)	0.2404 (± 0.0087)	0.2404 (± 0.0086)
Xe	0.2399	0.2399 (± 0.0344)	0.2399 (± 0.0389)	0.2399 (± 0.0373)	0.2399 (± 0.0350)	0.2399 (± 0.0344)

cell VMR seen in Fig. 7, with additional contributions from uncertainties in the measured *m/z* 14 background from CG1 and calculations involving Xe. The revised calibration constants generated by this procedure are provided in the last column of Table 2, with resulting calibration cell VMR shown in Fig. 8 and listed in Table 4.

The possibility that a small air leak may have impacted EQ mix analysis and the original calibration constants used to retrieve martian atmospheric VMR suggests that the O_2 calibration constant, which is not exercised during calibration cell analyses, may also have been affected because terrestrial air contains ~21% O_2. Although we cannot calculate a precise adjustment to the O_2 calibration constant using CG1 and CG2 data, we can evaluate the potential impact of terrestrial air during EQ mix sampling based on the adjustments required for the CO_2 and N_2 calibration constants. The range of air contribution during EQ mix analysis suggested by the required CO_2 and N_2 adjustments restricts the corresponding change in the ratio of *m/z* 40 and 32 to factors of 1.001–1.009. The latter value would place the revised O_2 calibration constant just above the upper limit provided by its current uncertainty. We have thus adjusted the uncertainty on the O_2 calibration constant from ± 0.013 to ± 0.014, as shown in Table 2, to encompass this range of possibilities.

3.6. Isotope ratios

Other key results provided by the calibration cell experiments involved computation of CO_2 and Xe isotope ratios for the calibration gas. As the CG2 experiment experienced some signal instability at *m/z* 45 and 46 that compromised isotopic calculations, only CO_2 isotope results for the CG1 experiment are discussed. Calculation of nitrogen and argon isotope ratios were compromised by difficulties modeling background contributions from F-HC compounds and HCl produced by high chlorine contents of solid materials processed by SAM (Glavin et al., 2013), respectively, so no results for those isotope systems are presented.

3.6.1. CO_2 isotopes

SAM QMS data allow calculation of both carbon and oxygen isotope ratios of CO_2. They are reported as delta values ($\delta^{13}C$ and $\delta^{18}O$) that represent per mil deviations from reference standards:

$$\delta^{13}\,C = 1000\cdot[(^{13}C/^{12}C)_{sample}/(^{13}C/^{12}C)_{V-PDB} - 1] \quad (3)$$

and

$$\delta^{18}\,O = 1000\cdot[(^{18}O/^{16}O)_{sample}/(^{18}O/^{16}O)_{V-SMOW} - 1], \quad (4)$$

where the reference standard for carbon is Vienna Pee Dee Belemnite (V-PDB) and that for oxygen is Vienna Standard Mean Ocean Water (V-SMOW).

Carbon isotope ratios are computed by several methods during routine SAM atmospheric analyses. The most straightforward calculation involves the ratio of background-corrected signal observed at *m/z* 12 and 13, providing a direct measurement of $^{13}C/^{12}C$. However, those *m/z* were affected by interferences from F-HC compounds during the calibration cell experiments. Other methods for calculation of $^{13}C/^{12}C$ utilize the signal at *m/z* 45 and require correction for interferences from the isotopologue $^{12}C^{16}O^{17}O$. As this in turn requires knowledge of the oxygen isotopic composition, we will discuss those calculations first, then return to carbon isotopes.

Oxygen isotope ratios of CO_2 would nominally be computed from the signal observed at *m/z* 44 and 46. Due to detector saturation at *m/z* 44, however, the signal for the major isotopologue at *m/z* 44 must be estimated from *m/z* 22 using the calibration constant provided by Franz et al. (2015). Corrections to this estimation are required to account for widening of the peak area at *m/z* 22 since pre-flight calibration, as discussed in Franz et al. (2015). The average changes in relative peak areas on Mars compared to ground calibration at *m/z* relevant to VMR

calculations were factored into the revised calibration constants given by Franz et al. (2015). This approach is sufficient for addressing effects on VMR calculations but not for isotope ratios, in which we are interested in deviations at a much smaller scale. Thus changes in peak areas were not factored into the calibration constant for estimation of *m/z* 44 from 22 given by Franz et al. (2015) because optimal calculations of CO_2 isotope ratios are achieved by correcting for the actual ratios of peak areas in each individual experiment. This is accomplished by computing the normalized peak areas at *m/z* ± 0.4 for *m/z* 22 and 46 (or *m/z* 22 and 45 for carbon isotope ratios) and correcting the measured ratios according to the difference in this ratio compared to that observed during ground calibration.

Accurate calculation of oxygen isotope ratios from the signal thus estimated or observed at *m/z* 44 and 46 requires correction for isobaric interferences from isotopologues containing ^{17}O and ^{13}C. A correction algorithm was derived using an approach similar to that of previous workers (Coleman, 2004; Craig, 1957; Thode et al., 1949), yielding the following expression:

$$^{18}R = (F_{peak} \times m46/m44 - {}^{17}R^2 - 2 \cdot {}^{13}R \cdot {}^{17}R) / 2, \quad (5)$$

where $^{18}R = {}^{18}O/{}^{16}O$, F_{peak} is a correction factor for normalized peak areas described above, m46 is the signal observed at *m/z* 46, m44 is the estimated signal at *m/z* 44 based on the observed *m/z* 22, $^{17}R = {}^{17}O/{}^{16}O$, and $^{13}R = {}^{13}C/{}^{12}C$. For calibration cell analyses, these corrections incorporated values of ^{17}R and ^{13}R based on the known isotopic composition of CO_2 provided by measurements during ground calibration (Franz et al., 2014). For analyses of martian atmospheric data, iterations between carbon and oxygen isotope ratio calculations, with the assumption that $\Delta^{17}O = 0.32\%$ for Mars (Franchi et al., 1999), are performed until convergence is achieved for ^{17}R and ^{13}R values.

A similar approach yielded the following expression for calculation of carbon isotope ratios from *m/z* 22 and 45:

$$^{13}C = (F_{peak} \times m45/m44 - 2 \cdot {}^{17}R), \quad (6)$$

where F_{peak} is a correction factor for normalized peak areas as described above, m45 is the signal observed at *m/z* 45, m44 is the estimated signal at *m/z* 44 based on the observed *m/z* 22, and $^{17}R = {}^{17}O/{}^{16}O$ expected for calibration cell, as before.

Prior to derivation of the algorithm to correct for pressure effects in production of CO_2^{++} ions discussed in Franz et al. (2015), an expression was derived to allow calculation of CO_2 carbon isotopic composition from data observed at *m/z* 45 and 46 alone, with appropriate corrections for oxygen isotopic composition:

$$^{13}R = (m45 \cdot {}^{17}R^2 + 2 \cdot m45 \cdot {}^{18}R - 2 \cdot m46 \times {}^{17}R)/(m46 - 2 \cdot m45 \cdot {}^{17}R), \quad (7)$$

where relevant quantities are the same as those already defined for Eqs. (5) and (6). Corrections for relative normalized peak areas at *m/z* 45 and 46 may also be applied, but the QMS tuning at these *m/z* is quite similar and this correction usually changes results by only a few per mil or less. The expression in Eq. (7) was useful in cross-comparison between QMS and TLS measurements of $\delta^{13}C$ during the earliest SAM experiments on Mars (Mahaffy et al., 2013), when QMS analyses using *m/z* 45 and 46 relied upon TLS values for oxygen isotopic composition, and offers ongoing verification of $\delta^{13}C$ calculated from *m/z* 12 and 13 and *m/z* 22 and 45.

Calculation of the CO_2 isotopic composition from the calibration gas experiments was challenging due to the introduction of excess background from atmospheric CO_2 during volume expansions, as discussed in Section 3.4. This is illustrated in Fig. 9, which shows the $^{13}C/^{12}C$ ratio calculated during initial data analysis using the nominal proportional background model. It is evident in the figure that the $^{13}C/^{12}C$ of the calibration gas (actual $\delta^{13}C = -42.67 \pm 0.06\%$) was affected by introduction of progressively greater proportions of atmospheric CO_2 ($\delta^{13}C \approx 45\%$, Mahaffy et al., 2013) as the calibration gas pressure was decreased. This result is consistent with increasing background from

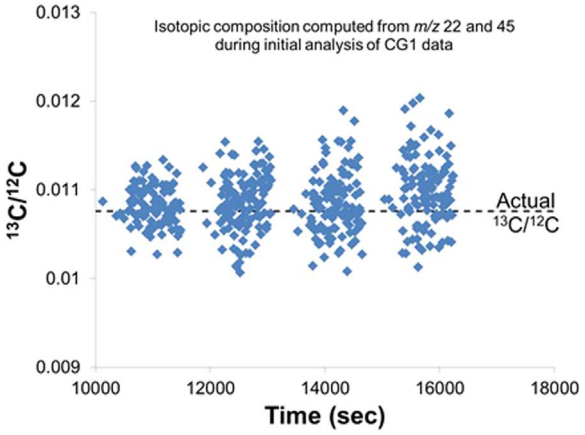

Fig. 9. CO_2 carbon isotopic composition measured during initial analysis of CG1 data at *m/z* 22 and 45. Error bars are omitted for clarity. The figure illustrates that as the calibration gas pressure decreased with successive volume expansions, the calculated $^{13}C/^{12}C$ rose due to increasing contribution from atmospheric gas in the background that was not properly removed, a finding consistent with initial VMR results indicating excess background CO_2.

atmospheric CO_2 apparent in VMR calculations, as discussed in Section 3.4. However, the isotopic composition determined for the highest pressure region of CG1, which was least affected by excess background, provides a coarse validation of the QMS capability to retrieve CO_2 isotope ratios. Application of the nominal proportional background model produced $\delta^{18}O$ of 7.0 ± 14.8% (compared to the actual $\delta^{18}O$ of 6.61 ± 0.06%), $\delta^{13}C$ of −36.3 ± 25.9% from *m/z* 22 and 45, and $\delta^{13}C$ of −40.6 ± 25.5% from *m/z* 45 and 46. Note that the uncertainties reported here include error propagation through all data corrections; the standard deviation of the mean for the measured ratios is approximately ± 2% for both $\delta^{13}C$ and $\delta^{18}O$. As the gas mixture in the manifold had already been altered by introduction of some atmospheric gas during the volume expansion prior to initial sampling of the calibration gas by the QMS, it is not surprising that these values reflect slight enrichments in heavy isotopes compared to the composition expected for the calibration gas due to the presence of atmospheric CO_2 that is not taken into account in this background model. Nevertheless, as the measured values of $\delta^{13}C$ and $\delta^{18}O$ match the expected values within ~6% or less despite inadequate correction for atmospheric gas in the background, these results validate the accuracy of QMS measurements of CO_2 isotope ratios.

Further validation of the measured CO_2 isotopic composition was achieved after correction for excess background gas by comparison of results for $\delta^{13}C$ and $\delta^{18}O$ obtained from *m/z* 22, 45 and 46 with those obtained for $\delta^{13}C$ from *m/z* 45 and 46 using the known oxygen isotopic composition for the calibration cell. This was accomplished by an extension of the VMR analysis described in Section 3.4. After subtraction of the *m/z* 22 background necessary to achieve the same signal in counts/mb as observed in the EQ mix experiment, the backgrounds at *m/z* 45 and 46 were calculated as those required for accurate retrieval of $\delta^{13}C$ and $\delta^{18}O$ from *m/z* 22, 45 and 46. Using these same background values, $\delta^{13}C$ was calculated from *m/z* 45 and 46 for comparison. In all four pressure regimes of CG1, this effort produced an error of ~3% or less in the $\delta^{13}C$ obtained from *m/z* 45 and 46, a value well within the uncertainty typically determined for QMS measurements of $\delta^{13}C$ and $\delta^{18}O$ that provides a constraint on the magnitude of mass discrimination at CO_2 isotopologues.

3.6.2. Xe isotopes

Calculation of Xe isotope ratios from QMS data is nominally straightforward, as described by Conrad et al. (2016), with ratios of background-subtracted signal at relevant *m/z* requiring only a correction for mass discrimination. The background at each relevant *m/z* was

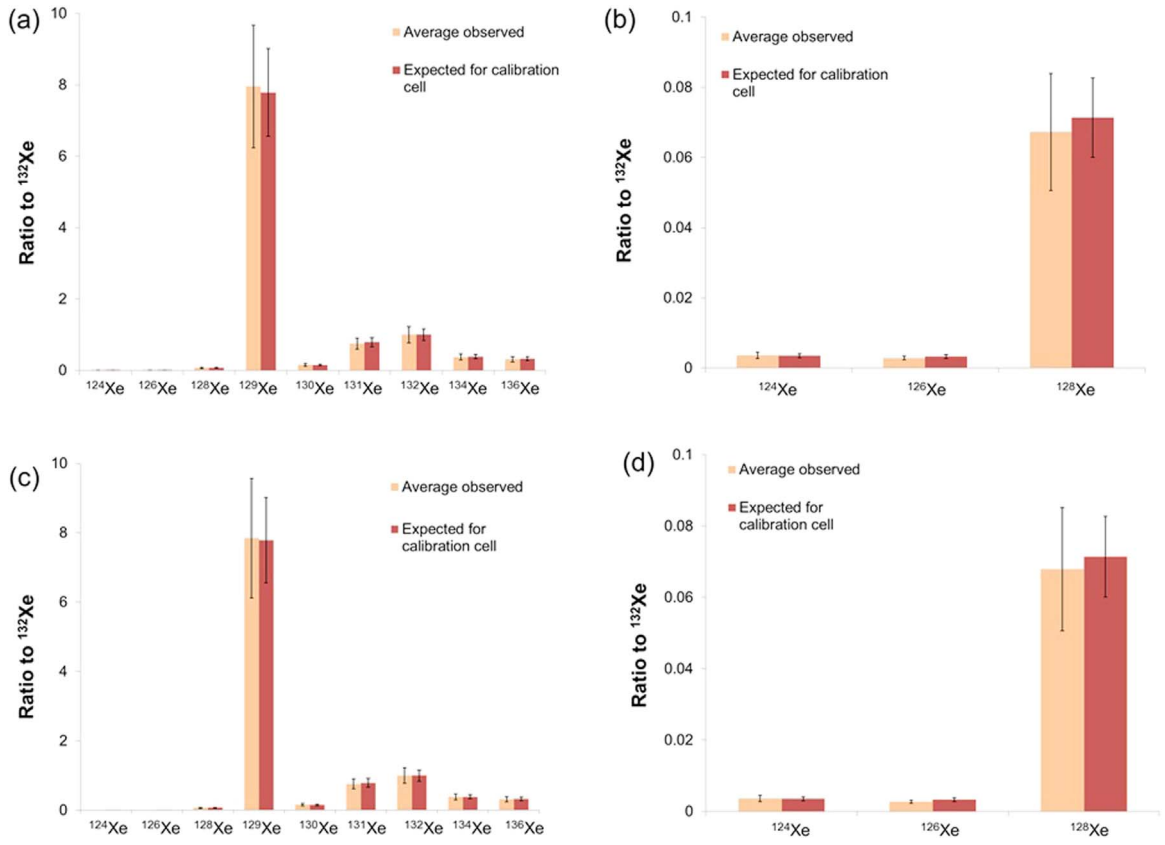

Fig. 10. Xe isotope ratios measured for the calibration cell experiments. (a) All isotopes, CG1; (b) Detail of minor isotopes, CG1; (c) All isotopes, CG2; (d) Detail of minor isotopes, CG2. Error bars on observed values include uncertainties associated with F-HC corrections and are thus larger than those for measurements of atmospheric Xe.

Table 5
Effects of applying revised N_2 calibration constant to VMR calculations for data acquired on MSL sols 45 and 77 (at solar longitudes of 175° and 193°, respectively).

Species	VMR with refined calibration constants (Franz et al., 2015)	Revised VMR with modified calibration constants[a]
CO_2	0.957(± 0.016)	0.949(± 0.016)
N_2	0.0203(± 0.0003)	0.0279(± 0.0005)
Ar	0.0207(± 0.0002)	0.0208(± 0.0002)
O_2	$1.73(\pm 0.06) \times 10^{-3}$	$1.74(\pm 0.06) \times 10^{-3}$
CO	$7.94(\pm 0.026) \times 10^{-4}$	$7.47(\pm 0.026) \times 10^{-4}$
$^{40}Ar/^{14}N$	0.51 ± 0.01	0.37 ± 0.01

[a] Weighted mean and associated uncertainty for each compound.

based on the background at *m/z* 132 computed during VMR calculations, assuming the same relative abundance compared to *m/z* 132 as measured at the start of the experiment, before correction for F-HC compounds. This method was devised in an effort to account for potential contributions from both Xe and F-HC compounds in the background. As described in Section 3.2, Xe isotopic analyses of data from the calibration cell experiments required additional corrections to account for isobaric interferences from F-HC compounds and temperature differences between ground calibration and experiments on Mars, listed in Table 3. All ratios are also corrected for differences in normalized peak areas, as already discussed for CO_2 isotopes above.

Fig. 10 shows the average of Xe isotope ratios measured for multiple pressure regimes of each experiment, after applying corrections for F-HC compounds. Error bars incorporate uncertainties in the F-HC correction factors and are therefore larger than those for enrichment experiments measuring Xe in the atmosphere (Conrad et al., 2016). As seen in the figure, all measured ratios are within uncertainty of those expected for the calibration cell, validating the QMS capability to measure Xe isotope ratios.

4. Implications for martian atmospheric composition

Because data from the atmospheric measurement regions of the CG1 and CG2 experiments were affected by high backgrounds due to residual calibration gas that compromised calculation of minor species, we do not report those results here. Rather, we assess the impact of the modified calibration constants given in Table 2 on the VMR retrieved for the martian atmosphere by reprocessing data acquired during two early SAM experiments reported previously (Franz et al., 2015; Mahaffy et al., 2013). These experiments (#25012 and #25027) were executed on sols 45 and 77 at solar longitudes of 175° and 193°, respectively. Results are given in Table 5, with previously reported results utilizing calibration constants described in Section 2.2 for comparison (Franz et al., 2015).

As expected, the N_2 VMR is impacted most significantly by the revised calibration constants, raising the weighted average for these two experiments to approximately 2.8 vol%. The weighted average for Ar VMR is approximately 2.1 vol%. When normalized to average annual pressure to remove seasonal effects due to the CO_2 condensation-sublimation cycle (Harri et al., 2014), the resulting N_2 and Ar VMR of 2.6 vol% and 1.9 vol%, respectively, may be compared with those reported for Viking measurements (Owen et al., 1977; Oyama and Berdahl, 1977). With or without pressure normalization, the average revised ratio of $^{40}Ar/^{14}N$ for these two experiments is 0.37 ± 0.01, a value between the previously reported SAM result of 0.51 ± 0.01 (Franz et al., 2015; Mahaffy et al., 2013) and the values of 0.3 (Owen et al., 1977) and 0.35 ± 0.08 (Oyama and Berdahl, 1977) reported for multiple Viking instruments.

It is of interest to compare SAM results for $\delta^{15}N$ vs. $^{40}Ar/^{14}N$ with those observed in martian atmospheric gas released through thermal processing of meteorite shock melt glasses, as shown in Fig. 11. This figure illustrates a linear trend in composition of gas trapped in glasses

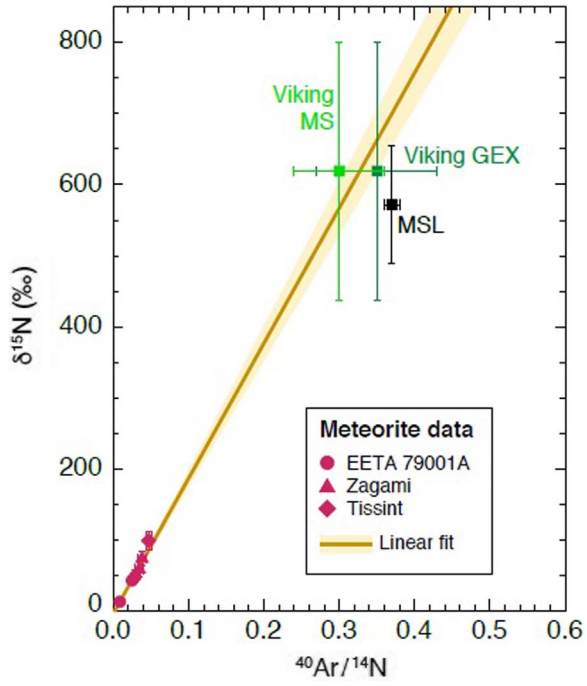

Fig. 11. Comparison of linear trend in spallation-corrected $\delta^{15}N$ vs. $^{40}Ar/^{14}N$ data for meteorite glasses (references given in text) with atmospheric measurements by two Viking instruments and SAM. For SAM, $^{40}Ar/^{14}N$ reported in this manuscript is plotted with $\delta^{15}N$ of Wong et al. (2013).

of the Zagami (Marti et al., 1995), EET 79001 (Becker and Pepin, 1984; Wiens et al., 1986), and Tissint (Aoudjehane et al., 2012) meteorites. The close agreement between this extrapolated trend and martian atmospheric composition as measured by the Viking Gas Exchange Experiment (GEX) (Oyama and Berdahl, 1977) leads to the interpretation that it represents a mixing line between indigenous crustal gas and martian atmospheric gas (Wiens et al., 1986). SAM measurements with the revised value for $^{40}Ar/^{14}N$ reported here overlap with those of Viking GEX, although not quite concordant with the meteorite data. As discussed by Wong et al. (2013), while a temporal trend toward enrichment in martian atmospheric $\delta^{15}N$ is well-modeled by escape processes, there is no known mechanism that could produce variability in atmospheric $^{40}Ar/^{14}N$, certainly at the time scale of repeated sampling by Viking and SAM. The intriguing possibility of variability in $\delta^{15}N$ driven by presently unknown or poorly understood processes provides motivation for the design of SAM experiments optimized to measure the nitrogen isotopic composition of solid surface materials, currently in development.

Acknowledgments

This work was funded by the NASA Mars Exploration Program. Data from all SAM experiments are archived in the Planetary Data System (pds.nasa.gov).

References

Aoudjehane, H.C., et al., 2012. Tissint martian meteorite: a fresh look at the interior, surface, and atmosphere of Mars. Science 338, 785–788.
Becker, R.H., Pepin, R.O., 1984. The case for a martian origin of the shergottites - Nitrogen and noble gases in EETA 79001. Earth Planet. Sci. Lett. 69, 225–242.
Coleman, M., 2004. Data corrections for mass-spectrometer analysis of SO_2. In: de Groot, P. (Ed.), Handbook of Stable Isotope Analytical Techniques.. Elsevier, Amsterdam.
Conrad, P.G., et al., 2016. In situ measurement of atmospheric krypton and xenon on Mars with Mars Science Laboratory. Earth Planet. Sci. Lett. 454, 1–9.
Craig, H., 1957. Isotopic standards for carbon and oxygen and correction for mass-spectrometric analysis of carbon dioxide. Geochim. Cosmochim. Acta 12, 133–149.
Franchi, I.A., et al., 1999. The oxygen-isotopic composition of Earth and Mars. Met. Planet. Sci. 34, 657–661.
Franz, H.B., et al., 2014. Analytical techniques for retrieval of atmospheric composition with the quadrupole mass spectrometer of the Sample Analysis at Mars instrument suite on Mars Science Laboratory. Planet. Space Sci. 96, 99–113.
Franz, H.B., et al., 2015. Reevaluated martian atmospheric mixing ratios from the mass spectrometer on the Curiosity rover. Planet. Space Sci. 109–110, 154–158.
Glavin, D.P., et al., 2013. Evidence for perchlorates and the origin of chlorinated hydrocarbons detected by SAM at the Rocknest aeolian deposit in Gale Crater. J. Geophys. Res. 119, 1–19.
Harri, A.M., et al., 2014. Pressure observations by the Curiosity rover: initial results. J. Geophys. Res. 119, 82–92.
Mahaffy, P.R., et al., 2012. The Sample Analysis at Mars investigation and instrument suite. Space Sci. Rev. 170, 401–478.
Mahaffy, P.R., et al., 2013. Abundance and isotopic composition of gases in the martian atmosphere from the Curiosity rover. Science 341, 263–266.
Marti, K., et al., 1995. Signatures of the martian atmosphere in glass of the Zagami meteorite. Science 267, 1981–1984.
Owen, T., et al., 1977. The composition of the atmosphere at the surface of Mars. J. Geophys. Res. 82, 4635–4639.
Oyama, V.I., Berdahl, B.J., 1977. The Viking gas exchange experiment results from Chryse and Utopia surface samples. J. Geophys. Res. 82, 4669–4676.
Thode, H.G., et al., 1949. Natural variations in the isotopic content of sulfur and their significance. Can. J. Res. 27, 361–373.
Webster, C.R., Mahaffy, P.R., 2011. Determining the local abundance of martian methane and its $^{13}C/^{12}C$ and D/H isotopic ratios for comparison with related gas and soil analysis on the 2011 Mars Science Laboratory (MSL) mission. Planet. Space Sci. 59, 271–283.
Wiens, R.C., et al., 1986. The case for a martian origin of the shergottites, II. Trapped and indigenous gas components in EETA 79001 glass. Earth Planet. Sci. Lett. 77, 149–158.
Wong, M.H., et al., 2013. Isotopes of nitrogen on Mars: atmospheric measurements by Curiosity's mass spectrometer. Geophys. Res. Lett. 40, 6033–6037.